High temperature structural and magnetic properties of cobalt nanorods

Kahina Ait Atmane, Fatih Zighem, Yaghoub Soumare, Mona Ibrahim, Rym Boubekri, Thomas Maurer, Jeremie Margueritat, Jean-Yves Piquemal, Frédéric Ott, Gregory Chaboussant, et al.

High temperature structural and magnetic properties of cobalt nanowires.

Kahina Ait Atmane,[a] FatihZighem,[b,†] YaghoubSoumare,[a] MonaIbrahim,[c] RymBoubekri,[c] ThomasMaurer,[b,†] JérémieMargueritat,[a,†] Jean-YvesPiquemal,[a,*] FrédéricOtt,[b] GrégoryChaboussant,[b] FrédéricSchoenstein,[d] NoureddineJouini[d] and GuillaumeViau,[c,*].

[a]Univ. Paris Diderot, Sorbonne Paris Cité, ITODYS, UMR CNRS 7086, 15 rue J.-A. de Baïf, 75205 Paris cedex 13, France.
[b]Laboratoire Léon Brillouin, CEA CNRS UMR 12, IRAMIS, CEA-Saclay, 91191 Gif sur Yvette, France.
[c]Université de Toulouse, LPCNO, INSA CNRS UMR 5215, 135 av. de Rangueil, 31077 Toulouse cedex 4, France.
[d]LSPM, CNRS UPR 9001, Université Paris XIII, Institut Galilée, 99 av. J.-B. Clément, 93430 Villetaneuse, France.

Correspondingauthors :

* E-mail: jean-yves.piquemal@univ-paris-diderot.fr (J.-Y. Piquemal); gviau@insa-toulouse.fr (G.Viau)

PresentAddresses

† F. Zighem : Laboratoire des Sciences des Procédés et Matériaux, CNRS UPR 3407, Institut Galilée, 99 avenue Jean-Baptiste Clément, 93430 Villetaneuse, France.

T.Maurer: Laboratoire de Nanotechnologie et d'Instrumentation Optique, ICD CNRS UMR STMR 6279, Université de Technologie de Troyes, BP 2060, 10010 Troyes cedex, France.

J.Margueritat : Laboratoire de Physicochimie des Matériaux Luminescents, CNRS UMR 5620, Université Claude Bernard Lyon 1, Bât. Alfred Kastler, 10 rue Ada Byron, 69622 Villeurbanne cedex, France.

Abstract. We present in this paper the structural and magnetic properties of high aspect ratio Co nanowires (~10) at high temperatures (up to 623 K) using in-situ X ray diffraction (XRD) and SQUID characterizations. We show that the anisotropic shapes, the structural and texture properties are preserved up to 500 K. The coercivity can be modelled by $\mu_0 H_C = 2(K_{MC} + K_{shape})/M_S$ with K_{MC} the magnetocrystalline anisotropy constant, K_{shape} the shape anisotropy constant and M_S the saturation magnetization. H_C decreases linearly when the temperature is increased due to the loss of the Co magnetocrystalline anisotropy contribution. At 500K, 50% of the room temperature coercivity is preserved corresponding to the shape anisotropy contribution only. We show that the coercivity drop is reversible in the range 300 - 500 K in good agreement with the absence of particle alteration. Above 525 K, the magnetic properties are irreversibly altered either by sintering or by oxidation.

Keywords.nanowires, cobalt, polyol process, permanent magnets, thermal treatments.

1. Introduction

The last decade has seen numerous investigations on anisotropic inorganic nanoparticles such as nanowires and nanorods for their peculiar physical properties and new applications in optics, magnetism or electronics [1, 2]. Several physical and chemical methods have been developed to grow ferromagnetic nanowires. The most used consists in the electrochemical reduction of Fe, Co or Ni salts within the unixial pores of an alumina or a polycarbonate membrane to confine the metal growth [3]. In order to grow nanowires with a diameter below 10 nm, other solid hosts have been employed such as carbon nanotubes [4] or mesoporous silica [5]. Recently, cobalt nanowires with diameters below 5 nm embedded in epitaxial CeO_2 layers were obtained by pulsed-laser deposition [6]. Iron-boride nanowires with diameter in the range 5-50 nm were obtained by chemical vapour deposition [7]. Wet chemistry methods, for which the adsorption of long chain molecules at the metal particle surface is the driving force of the anisotropic growth, were developed for the synthesis of cobalt [8] and cobalt-nickel nanowires [9].

One interest of the ferromagnetic nanowires is that they can present hard magnetic properties due to their large shape anisotropy. Magnetic nanowires have been recently proposed as potential candidates for high-density magnetic recording [10], nanowire-based motors [11] and the bottom-up fabrication of permanent magnets[12]. Indeed, very high coercivity values were observed on assemblies of cobalt rods or wires obtained using wet chemistry, either by the polyol process [13] or by organometallic chemistry [14]. Composite materials of well aligned cobalt wires with a volume fraction of 50% could exhibit higher $(BH)_{max.}$values than AlNiCo or ferrite-based magnets [11]. The interest of these liquid phase processes for the synthesis of nanowires with hard magnetic properties lies in the possibility to produce wires combining very good crystallinity and small diameter. The cobalt wires synthesized by these chemical methods crystallize with ahcp structure with the c axis along the long axis of the wires [8, 15]. The coincidence of the shape anisotropy easy axis and the magneto-crystalline anisotropy easy axis reinforces the whole magnetic anisotropy [12, 14].

But even if progresses have been made in the synthesis of ferromagnetic nanowires exhibiting large coercivities at room temperature and in the understanding of their

magnetic properties [12, 13, 16-18], there is still a lack of information about the stability of both their structural and magnetic properties at high temperature (above room temperature) which is a key information for any practical use of these materials for the fabrication of rare-earth free permanent magnets. The scope of this communication is to determine whether the anisotropic structure and texture are modified at high temperature and consequently whether their magnetic properties, and especially their large coercivities, are preserved. At high temperature, metal wires generally undergo an irreversible transformation to chains of spheres, described as the Rayleigh instability [19, 20]. Thehigh aspect ratio of compacted wires may also be altered by sintering. A first study showed that the thermal stability of “organometallic” cobalt nanowires was dependent on the atmosphere under which the wires were annealed [21]. Fragmentation of cobalt wires into chains of cobalt particles due to the Rayleigh instability was avoided when the cobalt wires were annealed in high vacuum conditions [21].

In this paper we present the high temperature structural and magnetic properties of cobalt nanowires prepared by the polyol process using in-situ characterizations up to 623 K under different atmospheres. The temperature range of stability of these wires and the temperature dependence of their intrinsic magnetic properties are described.

2. Materials and methods.

2.1. Syntheses of Co nanowires.

$CoCl_2 \cdot 6H_2O$ (Alfa Aesar, 99.9%), $RuCl_3 \cdot xH_2O$ (Aldrich, 99.98 %), NaOH (Acros), 1,2-butanediol (Fluka, ≥ 98%), methanol (VWR, Normapur) and sodium laurate, $Na(C_{11}H_{23}COO)$ (Acros, 98%) were used without any further purification.

The cobalt laurate precursor, $Co^{II}(C_{11}H_{23}COO)_2$ was first prepared. In 100 mL of distilled water at 333 K, was dissolved sodium laurate (75 mmol; 16.7 g) and to this solution, was added an aqueous solution (38 mL) of cobalt(II) chloride (40 mmol, 10,0 g) pre-heated at 333K under vigorous stirring. This resulted in the formation of a purple precipitate which was vigorously stirred at 333K for 15 min. The Co(II) solid phase was washed twice with distilled water (100 mL) then with methanol (100 mL) and finally dried in an oven at 323 K overnight. Yield: 94 % (based on Co).

The synthesis of the cobalt nanowires was realized according to a procedure previously described [13]. To 75.0 mL of 1,2-butanediol were added $Co(C_{11}H_{23}COO)_2$ (2.75 g, 0.08 M), $RuCl_3 \cdot xH_2O$ ($3.2\ 10^{-2}$ g) and NaOH (0.225 g, 0.075 M). The mixture was heated to 448 K with a ramping rate of 13 $K.min^{-1}$ for 20 min until the color of the solution turned black, indicating the reduction of Co(II) into metallic cobalt. After cooling to room temperature, the Co nanowires were recovered by centrifugation at 8500 r.p.m. for 15 min, washed with 50 mL of absolute ethanol (3 times), and finally dried in an oven at 323 K. Yield: 92 % (based on Co).

2.2. Preparation of the sample for magnetic measurements.

Two sets of samples were prepared for magnetic measurements: i) a few drops of a Co nanowires suspension in toluene were deposited on an aluminium foil and the toluene was removed by evaporation under the application of an external magnetic field of 1 T and ii) a pellet of magnetic nanowires was prepared using an infrared die (internal diameter 13 mm) and applying a pressure of about 6 tons delivered by a hydraulic press. The mass and the apparent density (including porosity) of the pellet were respectively 0.26 g and 2.13 g cm^{-3}. The true density of the powder, obtained at 298 K using a helium Accupyc 1330 pycnometer from Micromeritics, was found to be 6.76 $\pm$ 0.41 g cm^{-3}. The packing factor, defined as the ratio of the volume of the particles by the volume of the pellet was about 30%. Co nanowires are randomly oriented inside the pellet since no magnetic field was applied during its preparation.

2.3. Characterization techniques.

2.3.1. Room temperature characterizations.

Transmission electron microscopy (TEM) characterizations were performed using a Jeol 100-CX II microscope operating at 100 kV. Infrared spectra were recorded on a nitrogen purged Nicolet 6700 FT-IR spectrometer equipped with a VariGATR accessory (Harrick Scientific Products Inc., NY) fixing the incident angle at 62°. A drop of the colloidal solution was deposited on the Ge wafer and the spectrum was recorded when the solvent (absolute ethanol or toluene) was fully evaporated. XRD patterns obtained using Co K_α radiation (λ = 1.7889 Å) were recorded on a PANalyticalX'Pert Pro diffractometer equipped with an X'celerator detector in the range 20-80° with a 0.067° step size and 150 s per step. The size of coherent

diffraction domains, L_{hkl}, were determined using MAUD software which is based on the Rietveld method combined with Fourier analysis, well adapted for broadened diffraction peaks. Magnetic measurements were performed using a Quantum Design MPMS-5S SQUID magnetometer.

2.3.2. Thermal treatments and high temperature characterizations.

In order to follow the structural evolution of the samples with temperature, in-situ thermal treatments were realized in the range 300-673 K, using a HTK 1200N high-temperature X-ray diffraction chamber from Anton Paar. Two types of experiments were performed, depending on the oxygen content of the nitrogen gas used: in the first one, the powder was heated under a high-purity nitrogen atmosphere (O_2< 0.1 ppm; N_2Alphagaz 2) while in the second one, the oxygen content was substantially higher (O_2< 2 ppm; N_2Alphagaz 1). The samples were heated inside the high temperature X-ray diffraction chamber from room temperature to the final temperature using a 5 $K \cdot min^{-1}$ rate and maintained for 2 h at the final temperature before the acquisition of a X-ray diffraction pattern. Magnetization curves at high temperature were measured with a SQUID equipped with an oven. In this procedure the particles were heated in a reduced helium pressure.

3. Results and discussion.

3.1. Room temperature morphology, structure and magnetic properties of the cobalt particles.

TEM observations on the particles prepared by the polyol process showed Co nanowires with a mean diameter d_m = 13 nm and a mean length L_m = 130 nm (Figure 1a). The standard deviation of the diameter is very small (<15 % of the mean length) as it was observed before [13]. For the Co nanowires deposited on an Al substrate, the application of an external magnetic field results in the alignment of the cobalt anisotropic nanoparticles while the Co nanorods are randomly oriented within the pellet (see Figure 1b and 1c). Moreover Figure 1b shows also that the compression was not detrimental to the Co nanowires. The particles are ferromagnetic at room temperature and the coercivities measured for the Co nanoparticles deposited on the Al substrate and pressed into a pellet are respectively 530 and 230 mT (Figure 1d). The saturation magnetization of the wires is 113 emu g^{-1} (1.4×10^{-4} T m^3 kg^{-1}) and the M/M_S values forCo nanowires deposited on an Al substrate and pressed into a pellet

are respectively 0.67 and 0.46, indicating a higher degree of organisation in the former case, in agreement with the Stoner-Wholfarth model.Several parameters govern the coercivity of an assembly of anisotropic magnetic particles: (i) the distribution of the particle easy axis orientation with respect to the magnetic field and (ii) the particles shapes. For the cobalt wires we showed that the coercivity increases when they are aligned parallel to the applied magnetic field in good agreement with the Stoner-Wohlfarth model [13]. The coercivity is the sum of magnetocrystalline and anisotropy contributions. The contribution due to the shape anisotropy actually strongly depends on the detailed geometry of the wires and especially of the wire tips. This was investigated by micro-magnetic simulations [16]. On the one hand, while the ellipsoid shape is the most favourable, a cylindrical shape also provide a good shape anisotropy. On the other hand, enlarged tips create nucleation points for the magnetization reversal which can significantly reduce the coercivity by up to 30%. Surface effects related to the thin superficial CoO layer were extensively studied [18]. The measured Néel temperature of the CoO shell was 230 K. Significant modifications of the magnetic behaviour take place below this temperature. When the temperature decreases, a coercivity drop is actually observed below 150 K [18].

The Co nanowires were further characterized using TG-DT analyses under pure N_2 (O_2< 0.1 ppm). The thermogram (see Figure 2) showed a 7 % weight loss at about 575 K associated with a sharp endothermic peak. This weight loss is attributed to the elimination of organic matter adsorbed on the particle surface. Infrared spectroscopy was thus performed on the cobalt particles to characterize the organic matter remaining after the synthesis and the washing procedure at room temperature. The cobalt particle infrared spectrum washed twice with ethanol (Figure 3) exhibits a large band centered at 3300 cm^{-1} corresponding to the O-H stretching vibration. The OH groups can belong to a surface cobalt hydroxide and/or to adsorbed ethanol. At 2850 and 2920 cm^{-1} the symmetric and asymmetric C-H stretching vibration are respectively observed, which is attributed to the CH_2 groups of the laurate ions. In the region between 1400 and 1550 cm^{-1} the intense bands are attributed to the asymmetric and symmetric C-O stretching vibration of carboxylate groups, indicating that laurate ions remain at the particle surface. The intensity of all these bands decreases with the successive washings (Figure 3) showing that the amount of organic ligands at the particle surface is strongly dependent on the way they have been washed.

3.2. High temperature structural and chemical modification.

In order to follow the structural modifications of the nanowires when they are heated up, in-situ X-ray diffraction have been performed on Co nanowires for different temperatures ranging from 298 K up to 623 K. Ex-situ TEM analyses have also been realized for samples thermally treated in a tubular furnace using the same conditions. The structural and chemical modifications were found to depend on the atmosphere under which the cobalt wires are annealed.

3.2.1. N_2 atmosphere with O_2 concentration < 2 ppm.

Figure 4a shows the in-situ X-ray diffraction patterns of the Co nanowires annealed under a N_2 atmosphere at different temperatures. The results show that in spite of a small O_2 concentration (< 2 ppm), there is a progressive oxidation of the nanowires emphasized by the growth of the CoO (111) peak around 42°. With increasing temperature, the very broad peaks of the oxide becomes thinner indicating grain growth processes and/or crystallization of a pre-existing amorphous phase. Previous HRTEM studies performed on Co nanowires have evidenced the presence of a CoO layer composed of disoriented crystallites of various sizes [18], indicating that the former case is the more probable one. No structural modification was observed on the hcpnon oxidized cobalt phase.

3.2.2. N_2 atmosphere with O_2 concentration < 0.1 ppm.

For Co samples treated under N_2 with very low dioxygen content, the X-ray diffraction data show that there is also development of the CoO oxide between 298K and 473 K.Then, between 473 and 523 K, CoO vanished at the benefit of metallic Co as indicated by the sharpening and the increase of intensity of the Co peaks. For higher temperatures, 573 K and 623 K, CoO is detected again. Given the high temperature applied, the very low dioxygen content (0.1 ppm) is nevertheless sufficient to induce the formation of this oxide. For the as-synthesized sample, TG-DT analyses realized under N_2 (O_2 content 0.1 ppm) have shown a weight loss of about 7 % at 573 K associated with an endothermic signal (see Figure 2). This weight loss is explained by the decomposition of the remaining metal-organic species adsorbed at the particle surface. Indeed, IR-ATR experiments (Figure 3) have clearly shown vibrations

attributed to adsorbed laurate species (see above). These results suggest that the organic molecules remaining at the particle surface reduce the CoO shell in the temperature range corresponding to their decomposition. This effect can be evidenced only when the oxygen concentration in the atmosphere is small enough.

3.3. High temperature texture modification.

The XRD diffractograms showed that the hexagonal close-packed structure of the Co core is preserved for temperatures up to 623 K, whatever the annealing atmosphere. Nevertheless, a close examination of these patterns shows that the line broadening is modified during the thermal treatment. The mean crystallite sizes for the (10.0) and (00.2) reflexions have been determined and plotted as a function of the temperature treatment for samples annealed in $N_2$with the lowest oxygen content (Figure 5). At room temperature, the mean crystallite size for the (10.0) reflexion is always found much smaller than the mean crystallite size for the (00.2) reflexion. This observation confirms that the long axis of the cobalt wires is the c axis of the hcp structure. The data show that up to 500 K, the (10.0) and (00.2) mean crystallite sizes are more or less constant, indicating that the anisotropic shape of the crystallites is preserved. Major texture modifications are observed above 525K. Indeed, at this temperature a considerable increasing of both the $L_{10.0}$ and $L_{00.2}$ mean crystallite sizes is observed and the crystallites lose their anisotropy. At 525 K particles start to undergo sintering. In order to probe a possible deterioration of the Co nanowire morphology, TEM was performed for the samples treated at different temperatures. Figures 6a and 6b indicate that the shape of the nanowires is kept up to 523 K. On the other hand, Figure 6c shows that at 573 K and above, the nanowires start to sinter so that their shape anisotropy starts to fade away at these temperatures. At 623 K, the anisotropic shape is lost and only large aggregates are observed (Figure 6d). The sintering of the particles is probably enhanced by the fact that the CoO layer which likely acts as a protective layer preventing sintering has vanished at about 523 K (as seen by XRD, Figure 4b).

3.4. Magnetic properties at high temperature.

The high temperature magnetometry measurements were carried out on two types of cobalt samples: (A) particles washed with ethanol and pressed into pellets; (B)particles washed twice in ethanol and twice in toluene and deposited from a

diluted suspension in toluene onto an aluminium foil under a static magnetic field of 1 T to orient the cobalt wires during the drying process (see Fig. 1b). One has to keep in mind that the sample (A) contains more metal-organic matter than the sample (B). This difference can have a strong effect on the surface state at room temperature and on their chemical reactivity at high temperature.

Figure 7a presents the saturation magnetization normalized to the room temperature saturation magnetization, $M_S(T)/M_S(300K)$, as a function of temperature for samples (A) and (B). Two very different behaviors are observed. The saturation magnetization, M_S, of the sample (A) (pressed pellet) is rather stable up to 550 K: M_S only decreases by less than 1% from 300 K to 550 K. At 550 K, a jump of the magnetization is observed (Figure 7a). At higher temperatures (up to 800 K), the saturation magnetization decreases only moderately (10%). The magnetization jump at 550 K is irreversible. When the sample is cooled down to room temperature the magnetization is increased by 25% with respect to the initial room temperature value. The jump of the magnetization at 550K can be explained by the fact that the saturation magnetization of the Co initial pellet is 113 emu g^{-1} (1.4×10^{-4} T m^3 kg^{-1}) corresponding to only 70% of the bulk metal values. Such a low value is due to the surface oxidation of the wires and by the remaining organic matter in the pellet. The apparent density of the pellet, determined using He pycnometry, was found to be 6.76 ± 0.41 g cm^{-3} (see experimental section). Taking into account that the organic matter in the particles corresponds to about 7 wt. % and that the CoO layer thickness is 1.2 nm for a nanowire with a mean diameter of 15 nm and a mean length of 130 nm [18], the ratio of the mass of Co to the total mass of the solid (including CoO and the organic matter) can be estimated. The determined value, 73 wt. % is in excellent agreement with that determined using the M_S value.Thus, the jump of magnetization at 550 K can be explained by the decomposition of remaining metal-organic at the surface of the nanowires that reduces the cobalt oxide layer and causes the apparition of added metallic Co. This phenomenon was clearly evidenced by XRD (Figure 4b). For the sample (B), the saturation magnetization of the cobalt wires washed vigorously and deposited on an aluminium foil from a diluted suspension varies only slightly up to 500 K but decreases strongly above this temperature. In this case, the decrease of the magnetization is explained by the oxidation of the cobalt wires into CoO as was inferred by XRD in the case of the experiment presented on

Figure 4a. The successive washings have removed most of the organic matter (Figure 3) and no reduction can occur. The He reduced pressure in the oven of the SQUID is not enough to prevent the powders from oxidation at high temperature.
Figure 7b presents the coercivity normalized to the room temperature coercivity, $H_C(T)/H_C(300K)$ as a function of temperature for the same samples (Co pellets, on one hand, and washed Co wires deposited on an Al foil, on the other hand). In the temperature range 300-500K the two samples exhibit the same magnetic behavior: the coercivity decreases linearly when the temperature increases and, in both cases, the coercivity at 500K is about 50% of the value at 300K. It is important to stress that the two samples do not have the same coercivity at room temperature: the value of the oriented cobalt wires, 530 mT, is much higher than that of the pressed pellet, 230 mT, in which the wires are randomly oriented. It is noteworthy that despite this difference, the coercivities normalized to the room temperature values follow the same behavior. This decrease is independent on the wire dispersion but is an intrinsic property of cobalt. As it will be described more precisely in the next section, this behavior is related to the temperature dependence of hcp cobalt.

Above 500 K two different behaviors are observed depending on the sample preparation procedure. The coercivity of the cobalt pellets collapses and becomes negligible at 550 K while the coercivity of the cobalt wires deposited on the Al foil still follows a linear decrease between 500 and 600 K (Figure 7b). In the first case, sample (A), the cobalt wires undergo a sintering in the temperature range corresponding to the decomposition of the metal-organic matter and to the reduction of the surface cobalt oxide. The cobalt particles lose their anisotropy as it was observed on the textural analysis of the XRD patterns (Figure 5). Thus, the very small coercivity value is explained by the vanishing of the magnetic shape anisotropy due to sintering and by a weakmagnetocrystalline anisotropy of cobalt at 550 K (see next section). On the other hand, the cobalt wires washed and deposited, sample (B), undergo a slow oxidation as was inferred from the decrease of the saturation magnetization. In this latter case, the magnetic shape anisotropy is preserved up to 600 K. No sintering occurs probably for several reasons: the wires are much more isolated on the foil than in the pellet, the amount of organic matter is much lower and the surface oxidation prevents wires coalescence.

Nanowire oxidation and surface reduction are irreversible processes. However, we have checked that when the wires are heated below 500K both the magnetization and the coercivity variation are reversible. The samples recover their initial magnetization and coercivity when they were cooled down to room temperature. Therefore, these nanowires can be annealed at temperatures as large as 500 K without losing their shape anisotropy. However to reach higher treatment temperatures, these objects would need to be separated from each other to prevent sintering.

3.4.1. High temperature evolution of the coercive field.

A linear temperature dependence of the coercivity was observed for the sample (B), i.e. Co wiresdeposited on an aluminium foil (Figure 7b). Between 300 and 600K, as far as particle sintering is avoided, the coercivity $\mu_0 H_C$ (mT) can be expressed as:

$$\mu_0 H_C / \mu_0 H_C(300K) = 1 - a(T - 300) \qquad (1)$$

where$\mu_0 H_C$(300K), the room temperature coercivity is 530 mT and *a* is 2.4×10^{-3} $K^{-1}$for Co nanoparticles. As shown in Figure 8, the magneto-crystalline anisotropy constant K_{MC} of bulk hcp Co is almost temperature independent from 0 to 200 K and linearly decreases from $K_{MC}\approx 6.6\times10^{5} J.m^{-3}$ at 200 K down to $K_{MC}\approx -1.2\times10^{5} J.m^{-3}$ at 600 K [22-24].A positive K_{MC} value corresponds to an easy axis along *c*, i.e. along the wire axis. A negative K_{MC} value corresponds to an easy axis perpendicular to *c*, i.e. perpendicular to the wire axis. Note that, above 500 K, the value of the magnetocrystallineconstant becomes negative which means that it counteracts the shape anisotropy of the wire. The observed linear temperature drop of the coercivity is essentially related to the temperature dependence of the magnetocrystalline anisotropy of Co. At the opposite, the weak temperature dependence of the coercivity of cobalt wires grown by electrochemistry illustrates the dominance of shape anisotropy and the small magneto-crystalline contribution [25].

At a fixed temperature, within the Stoner-Wohlfarth model, the coercivity of elongated ellipsoidal particles with their long axis aligned with the applied field can be expressed as [26]:

$$\mu_0 H_C = 2(K_{MC} + K_{shape})/M_S \qquad (2)$$

whereK_{shape} corresponds to the effective anisotropy constant related to the shape anisotropy of the nanowires. Note that this formula is strictly valid only if the magnetization rotation is coherent, which requires that the nanowires diameter is very small (≈ 8 nm for Co). Our nanowires dimensions are close to this limit.

Magnetization measurements in the range 5 K to 500 K show that the magnetization is almost constant, within a few percents. Since the shape anisotropy is proportional to M_s, this allows us to make the assumption that the shape anisotropy contribution is constant over this range of temperatures. On the other hand, around 500 K, the Co magneto-crystalline anisotropy K_{MC} can be assumed to be close to zero, reducing the contribution of the magnetocrystalline anisotropy to the coercivity close to zero. The value of the coercivity normalized to the room temperature coercivity at 500 K, about 0.50 (see Figure 7b), allows to calculatethe coercivity at this temperature: $\mu_0 H_C \approx$ 260 mTwhich corresponds to the contribution of the shape anisotropy. This corresponds to only half of the theoretical value for an aspect ratio of 5 ($2K_{shape}/M_S \approx$ 527 mT) but is close to that of previous assessments ($2K_{shape}/M_S \approx$ 380 mT) obtained by fitting room temperature hysteresis curves [12]. The fact that the measured value is significantly smaller than the maximum theoretical value for equivalent ellipsoid can be easily accounted for by the fact that: (i) the assembly of wires is not well aligned which dramatically reduces the coercivity related to the shape anisotropy, (ii) for an equivalent aspect ratio, ellipsoids have a higher coercivity compared to cylinders because of domain nucleation [16]for the latter and (iii) we are not working at 0 K.

Using equation (2), it is possible to plot the $K_{MC}(T)$ dependence for the Co nanowires (see Fig. 8) We calculate $K_{shape} = \mu_0 H_C \times M_S/2 \approx 1.8 \times 10^5$ J m^{-3}, assuming M_S = 1.4 MAm^{-1}. Our experimental determination of the temperature dependence of K_{MC} leads to values smaller than that of the bulk Co. It can be accounted for by the angular distribution of the nanowires axis with the applied magnetic field which reduces the coercivity measured along the applied field [12]. Moreover, although our nanowires are well crystallized in the hcp phase [13], some stacking faults (fcc phase) can appear and can further reduce the value of K_{MC}. We may add that the value of the cobalt anisotropy constant is controversial because it suffers large variations in the literature [27, 28]. For example, in epitaxial Co hcp thin films, the value of the magnetocrystalline anisotropy is generally found to be half the value of the expected

one at room temperature. The deduced values of K_{MC} of our nanowires are thus not so smaller than the ones obtained in epitaxial Co thin films.

From a point of view of using Co nanowires as a basis for the fabrication of permanent magnetic materials, one important aspect was to evaluate magnetic dipolar magnetic interactions between nanowires in dense magnetic aggregates. This has been very recently addressed and micromagnetic simulations have shown that dipolar interaction between wires are not detrimental to the high coercivity properties, even for very dense aggregates [17].Dealing with the working temperature, the present study shows that the temperature dependence of the Co magneto-crystalline anisotropy may be a real limitation. K_{MC} not only vanishes around 500 K but becomes negative above this temperature, which, as a consequence, leads to magnetic properties which are very sensitive to the temperature. Nevertheless, the materials are rather resilient to high temperatures (up to 550K) and are competitive with the other existing types of permanent magnetic materials. The magnetic performances of Co nanowires are of the order of $(BH)_{max}\approx$ 12-15 MGOeat room temperature [12]which rank them in-between ferrites ($\approx$ 3 MGOe) and AlNiCo ($\approx$ 5 MGOe) and RE-magnets (NdFeB$\approx$ 40 MGOe; SmCo$\approx$ 20-30 MGOe). A general drawback of rare earth based materials is their relatively lower Curie temperature (580K for NdFeB and 1023K for SmCo) which leads to a significant dependence of the magnetization at high temperatures which is not the case for pure Co systems ($T_c\approx$ 1300K). NdFeB magnets cannot be operated at temperatures above 400 K because of irreversible losses. SmCo magnets can be operated at elevated temperatures (up to 523K typically) which is equivalent to our materials. They have a similar temperature coefficient for the coercive field ($\approx -2\times10^{-3}$ K^{-1}) as Co nanowires.

4. Conclusion.

The interest of high aspect ratio cobalt nanoparticles prepared by the polyol process lies in their well-controlled morphology, diameter smaller than 15 nm, high aspect ratio and shape homogeneity, and, consequently, in their high coercivity at room temperature. In this paper, we have presented a study on structural and magnetic properties of these particles at high temperatures.

In the temperature range 300-500 K, we show that the coercivity decreases linearly and that this variation is reversible. In this range no particle alteration occurs and the coercivity can be modelled by $\mu_0 H_C = 2(K_{MC} + K_{shape})/M_S$ with K_{MC} the magnetocrystalline anisotropy constant, K_{shape} the shape anisotropy constant and M_S the saturation magnetization. The K_{MC} constant being the only parameter responsible for the temperature dependence, high temperature magnetic measurements appear as a very simple method to evaluate the respective contribution of shape and magnetocrystalline anisotropy. At 500 K, 50% of the room temperature coercivity is maintained. This value corresponds to the contribution of the shape anisotropy to the global anisotropy while at 500K the magnetocrystallinecontribution has vanished. This value confirms previous numerical calculations.

Above 525 K,the magnetic properties are irreversibly altered either by sintering or by oxidation. In absence of oxygen the decomposition of metal-organic matter remaining at the particle surface reduces the native cobalt oxide layer and provokes coalescence.Thecoercivityis irreversibly altered by the loss of shape anisotropycorresponding to the transition for magnetic mono- to multi-domains particles (see Figure 5 and 6d). In slightly oxidative conditions, the growth of a thin oxide layer at the wire surface prevents from sintering but decreasessignificantlythe saturation magnetization

Above 500 K a sintering of the particles can occur that has been evidenced by TEM analysis and by in-situ XRD pattern analysis. This study clearly shows that this sintering is favoured by the presence of metal-organic matter remaining at the particle surface which reduces the thin cobalt oxide layer in the temperature range 525-575 K as was inferred by in-situ XRD measurements. The apparition of added metallic Co has for consequence to irreversibly increase the saturation magnetization of the particles but also to induce a collapse of the coercivitydue to sintering. Sintering was not observed when the main part of the organic matter was removed by washing; in that case the thin surface oxide layer avoids this phenomenon but oxidation decreases the wire magnetization. In terms of temperature stability some further work is necessary to prevent both coalescence and oxidation of the wires at high temperatures (>550K). The use of a passivation layer is a possible route to that.

Acknowledgements

The authors gratefully acknowledge the AgenceNationale de la Recherche for their financial support (project 07-NANO-009 MAGAFIL). We thank F. Herbst (ITODYS) for providing the TEM images of nanowires and J.B. Moussy (CEA-IRAMIS) for his help in the magnetometrymeasurements. The help of Dr. S. Khennache for Hepycnometry measurements was greatly appreciated.

References

[1] C. M. Lieber, Z. L. Wang,MRS Bull. 32 (2007) 99-.

[2] Y. N. Xia, P. D. Yang, Y. G. Sun, Y. Y. Wu, B. Mayers, B. Gates,Y. D. Yin, F. Kim, Y. Q. Yan, Adv. Mater. 15 (2003) 353-.

[3] D. J. Sellmyer, M. Zheng, R. Skomski, J. Phys. : Condens. Matter 13 (2001) R433-R460.

[4] (a) C. M. Tilmaciu, B. Soula, A. M. Galibert, P. Lukanov, L. Datas, J. Gonzalez, L. F. Barquin, J. R. Fernandez, F. Gonzalez-Jimenez, J. Jorge, E.Flahaut,Chem. Commun.43 (2009) 6664-6665; (b) U. Weissker, M.Loffler, F.Wolny, M. U.Lutz, N.Scheerbaum, R.Klingeler, T.Gemming, T.Muhl, A.Leonhardt, B.Buchner,J. Appl. Phys.106 (2009) 054909.

[5] (a) R. Campbell, M. G.Bakker, G.Havrilla, V. Montoya, E. A.Kenik, M.Shamsuzzoha, MicroporousMesoporous Mater. 97 (2006) 114; (b) M. V. Chernysheva, N. A.Sapoletova, A. A.Eliseev, A. V.Lukashin, Y. D.Tretyakov, P.Goernert, Pure and Appl.Chem. 78 (2006) 1749; (c) Z. Zhang, S.Dai, D. A.Blom, J.Shen, Chem. Mater.14 (2002) 965; (d) H. Luo, D. Wang, J.He, Y. Lu, J. Phys. Chem. B 109 (2005) 1919.

[6] (a) F. Vidal, Y. Zheng, J. Milano, D. Demaille, P. Schio, E. Fonda, B. Vodungbo,Appl. Phys. Lett.95 (2009) 152510 ; (b) P. Schio, F. Vidal, Y. Zheng, J. Milano, E. Fonda, D. Demaille, B. Vodungbo, J. Varalda, A. J. A. de Oliveira, V. H. Etgens Phys. Rev. B 82 (2010) 094436.

[7] Y. Li, E. Tevaarwerk, R. P. H.Chang,Chem. Mater. 18 (2006) 2552-.

[8] (a) F. Dumestre, B. Chaudret, C. Amiens, M.-C. Fromen, M.-J. Casanove, P. Renaud, P. Zurcher, Angew. Chem. Int. Ed. 41 (2002) 4286; (b) F. Dumestre, B.Chaudret, C. Amiens, M. Respaud, P. Fejes, P. Renaud, P. Zurcher, Angew. Chem. Int. Ed.42 (2003) 5213.

[9] Y. Soumare, J.-Y.Piquemal, T.Maurer, F.Ott, G.Chaboussant, A.Falqui, G. Viau, J. Mater. Chem. 18 (2008) 5696.

[10] (a) Y. Xie, J.-M. Zhang, J. Phys. Chem. Sol. 73 (2012) 530-534 ; (b) A. S. Samardak, E. V. Sukovatitsina, A. V. Ognev, L. A. Chebotkevich, R. Mahmoodi, S. M. Peighambari, M. G. Hosseini, F. Nasirpouri, J. Phys. : Conf. Ser. 345 (2012) 012011 ; (c) A. Morelos-Gómez, F. López-Urías, E. Muñoz-Sandoval, C. L. Dennis, R. D. Shull, H. Terrones, M. Terrones, J. Mater. Chem. 20 (2010) 5906-5914 ; (d) X. Huang, L. Li, X. Luo, X. Zhu, G. Li, J. Phys. Chem. C 112 (2008) 1468-1472.

[11] O. S. Pak, W. Gao, J. Wang, E. Lauga, Soft Matter 7 (2011) 8169-8181.

[12] T. Maurer, F. Ott, G.Chaboussant, Y. Soumare, J.-Y. Piquemal, G. Viau, Appl. Phys. Lett. 91 (2007) 172501.

[13]Soumare, Y. ; Garcia, C. ; Maurer, T. ; Chaboussant, G. ; Ott, F. ; Fiévet, F. ; Piquemal J-Y.; Viau, G. Adv. Funct. Mater. 2009, 19, 1971.

[14]Soulantica, K.; Wetz, F.; Maynadié, J.; Falqui, A.; Tan, R. P.; Blon, T.; Chaudret, B.; Respaud, M. Appl. Phys. Lett. 2009, 95, 152504.

[15] Viau, G.; Garcia, C.; Maurer, T.; Chaboussant, G.; Ott, F.; Soumare, Y.; Piquemal, J.-Y. Phys. StatusSolidi A 2009, 206, 663.

[16]Ott, F.; Maurer, T.; Chaboussant, G.; Soumare, Y.; Piquemal, J.-Y.; Viau, G. J. Appl. Phys. 2009, 105, 013915.

[17]Maurer, T.; Zighem, F.; Fang, W.; Ott, F.; Chaboussant, G.; Soumare, Y.; Ait Atmane, K.; Piquemal, J.-Y.; Viau, G. J. Appl. Phys. 2011, 110, 123924.

[18] Maurer, T.; Zighem, F.; Ott, F.; Chaboussant, G.; André, G.; Soumare, Y.; Piquemal, J.-Y.; Viau, G.; Gatel, C. Phys. Rev. B 2009, 80, 064427.

[19]Karim, S; Toimil-Molares, M.E.; Balogh, A.G.; Ensinger, W.; Cornelius, T.W.; Khan, E.U.; Neumann, R. Nanotechnology2006,17, 5954

[20]Nisoli, C.; Abraham, D.; Lookman, T.; Saxena, A. Phys. Rev. Lett.2009, 102, 245504.

[21]Ciuculescu, D.; Dumestre, F.; Comesaña-Hermo, M.; Chaudret, B.; Spasova, M.; Farle, M.; Amiens, C., Chem. Mater. 2009, 21, 3987.

[22] Carr, W.J. Phys. Rev. 1958, 109, R1971.

[23] Ono F.; Yamada, O. J. Phys. Soc. Jap. 1979, 46, 462.

[24] Ono, F. J. Phys. Soc. Jap. 1981, 50, 2564.

[25] Liu, Z.; Chang, P.-C.; Chang, C.-C.; Galaktionov, E.; Bergmann, G.; Lu, J.G. Adv. Funct. Mater.2008, 18, 1573.

[26] R. C.O'Handley, *Modern Magnetic Materials, Principles and Applications*, Wiley, New York, 2000, p. 319.

[27] C. Chappert, P. Bruno, J. Appl. Phys. 64 (1988) 5736.

[28] Y. Roussigné, F. Ganot, C.Dugautier, P. Moch,D. Renard, Phys. Rev. B 52 (1995) 350-.

Graphical Abstract

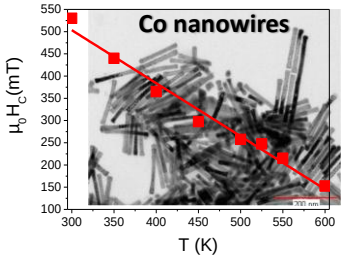

Figure Captions

Figure 1. TEM images of Co nanowires (L_m= 130 nm, d_m= 13 nm) (a); SEM images of Co nanowires deposited on an aluminium foil from several drops of a wires suspension in toluene with the application of an external magnetic field of 1T during the drying (b), of the surface of a pellet made of compressed Co nanorods(c) and magnetization curves at 300 K of the Co nanowires deposited on an aluminium foil and the Co pressed into a pellet (d). Inset: the Co nanowires are rather well aligned inside the elongated microscopic structures, with an angular dispersion on the order of σ = 7° [15].

Figure 2. Thermogravimetric and differential thermal analyses realized on Co nanowires under N_2 (O_2< 0.1 ppm).

Figure 3. Infrared absorption spectra of cobalt wires washed twice with ethanol (a); washed twice with ethanol and once (b), twice (c) and three times (d) with toluene.

Figure 4. In-situ X-ray diffraction patterns of Co nanowires thermally treated under N_2 with (a) low dioxygen content (O_2< 2 ppm) and (b) very low dioxygen content (O_2< 0.1 ppm). In each case, the hexagonal structure of Co is preserved up to the highest temperatures.

Figure 5. Variation of the $L_{10.0}$ and $L_{00.2}$ mean crystallite sizes with increasing temperature for Co samples treated under N_2 (O_2< 0.1 ppm).

Figure 6. TEM images of Co wires (a) after drying at 330 K and after thermal treatment under N_2 (O_2< 0.1 ppm) for 2 hours at 523 K (b), at 573 K (c) and 2 hours at 623 K (d).

Figure 7. Saturation magnetization to room temperature saturation magnetization ratio as a function of temperature (a) and coercivity normalized to the room temperature coercivity as a function of temperature (b) for a pellet of compacted cobalt nanowires washed only with absolute ethanol (□) and for cobalt nanowires washed twice with absolute ethanol and twice with toluene and deposited on an aluminium foil (•).The solid line is a linear fit to the experimental data corresponding to cobalt nanowires deposited on an aluminium substrate, which is given by $\mu_0 H_C(T) / \mu_0 H_C(300K) = 1 - a(T - 300)$ (see text for details).

Figure 8. Deduced temperature dependence of the magnetocrystalline anisotropy constant for the Co nanowires (red circles). The bulk values data (open circles) of K_{MC} have been reproduced from Refs. [21] and [22].

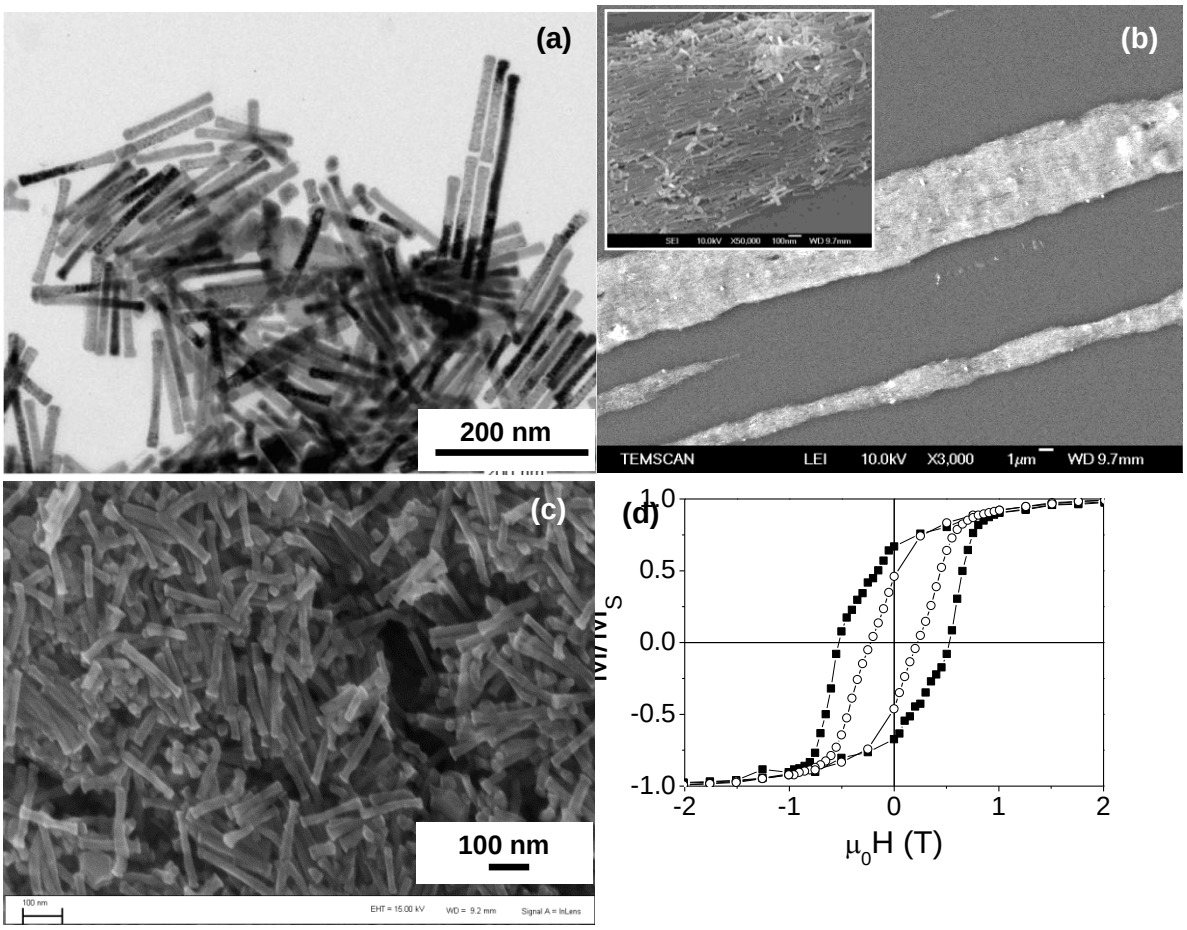
(a)
200 nm
(b)
TEMSCAN
LEI
10.0kV
X3,000
1μm
WD 9.7mm
(c)
100 nm
(d)
1.0
0.5
0.0
-0.5
-1.0
-2
-1
0
1
2
μ0H (T)

Figure 1.

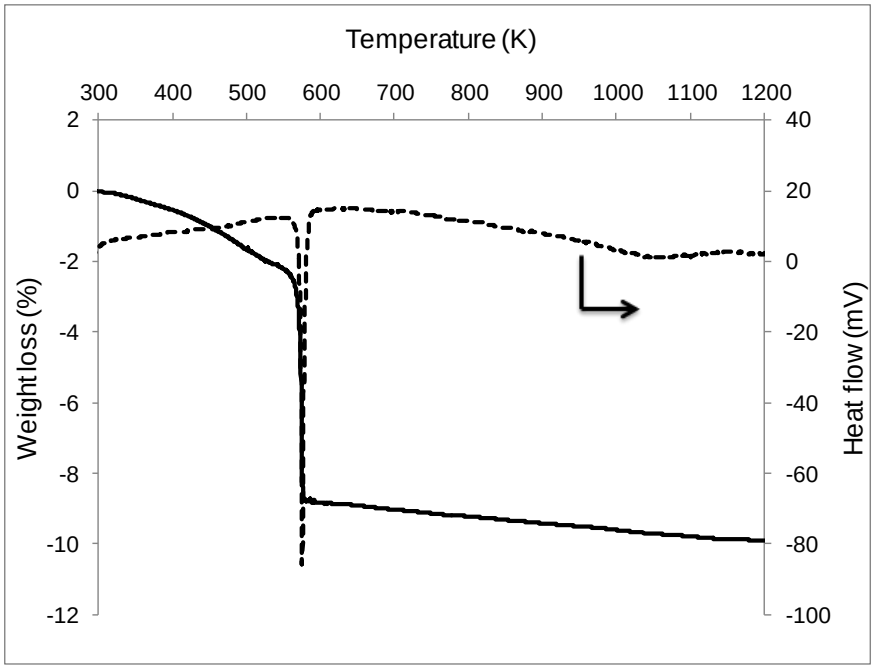
Temperature (K)
300
400
500
600
700
800
900
1000
1100
1200
2
0
-2
-4
-6
-8
-10
-12
40
20
0
-20
-40
-60
-80
-100
Weight loss (%)
Heat flow (mV)

Figure 2.

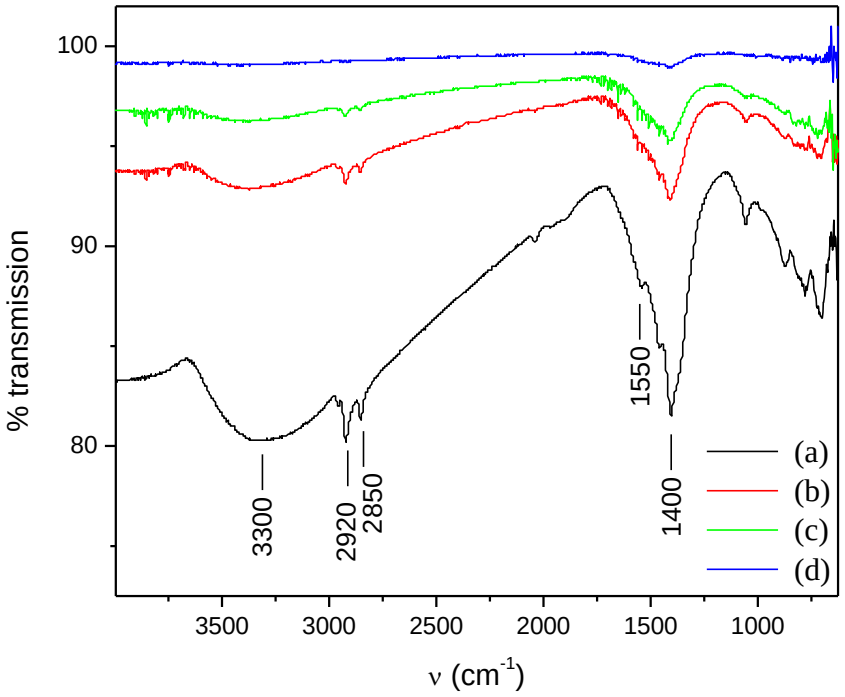
100
90
80
% transmission
3300
2920
2850
1550
1400
(a)
(b)
(c)
(d)
3500
3000
2500
2000
1500
1000
ν (cm-1)

Figure 3.

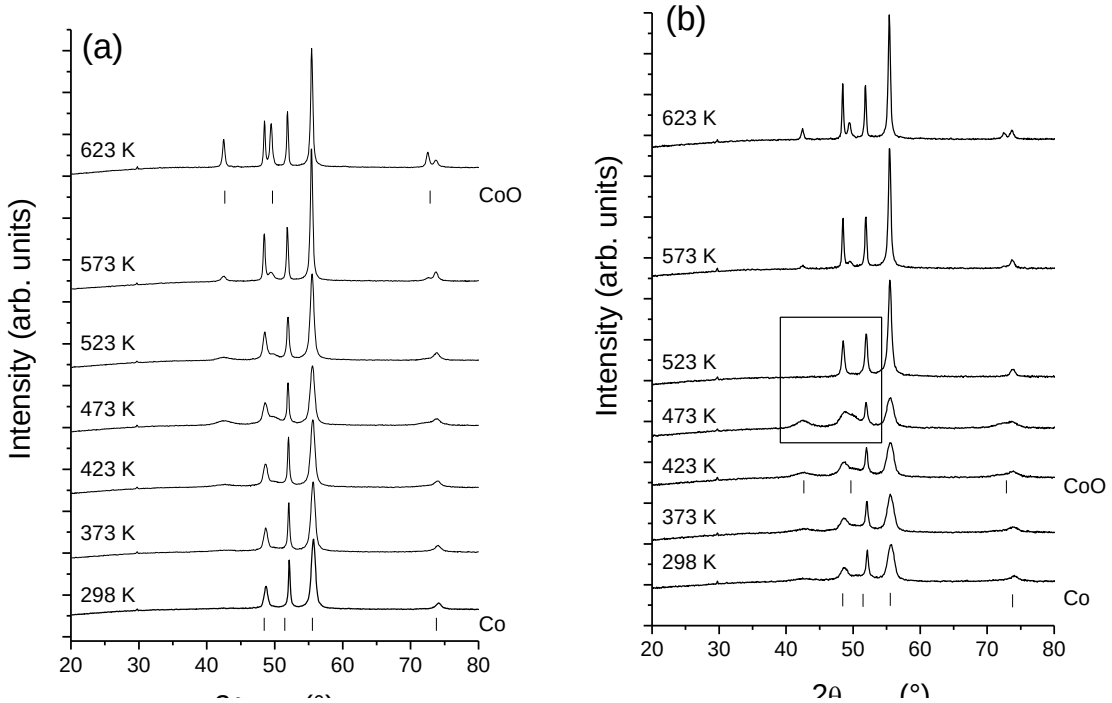
(a)
623 K
573 K
523 K
473 K
423 K
373 K
298 K
CoO
Co
Intensity (arb. units)
20
30
40
50
60
70
80
(b)
623 K
573 K
523 K
473 K
423 K
373 K
298 K
CoO
Co
Intensity (arb. units)
20
30
40
50
60
70
80

Figure 4.

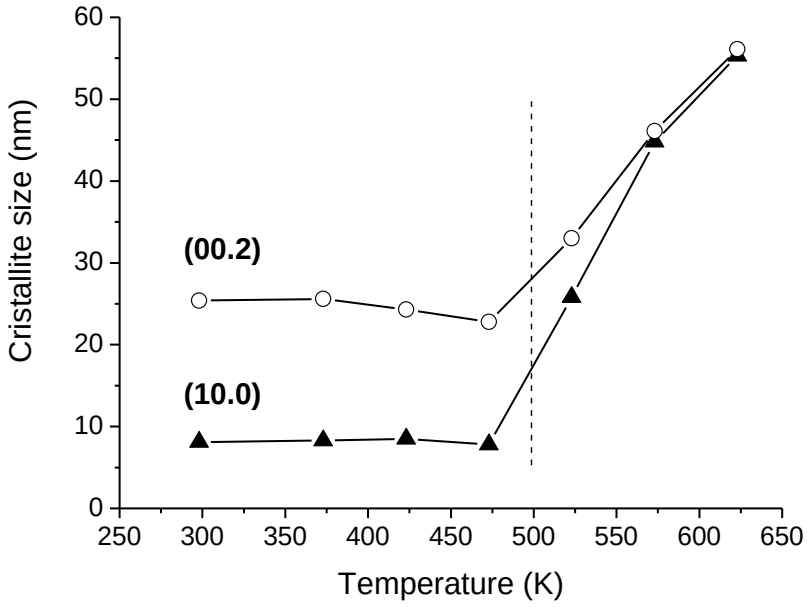
Cristallite size (nm)
Temperature (K)
(00.2)
(10.0)
0
10
20
30
40
50
60
250
300
350
400
450
500
550
600
650

Figure 5.

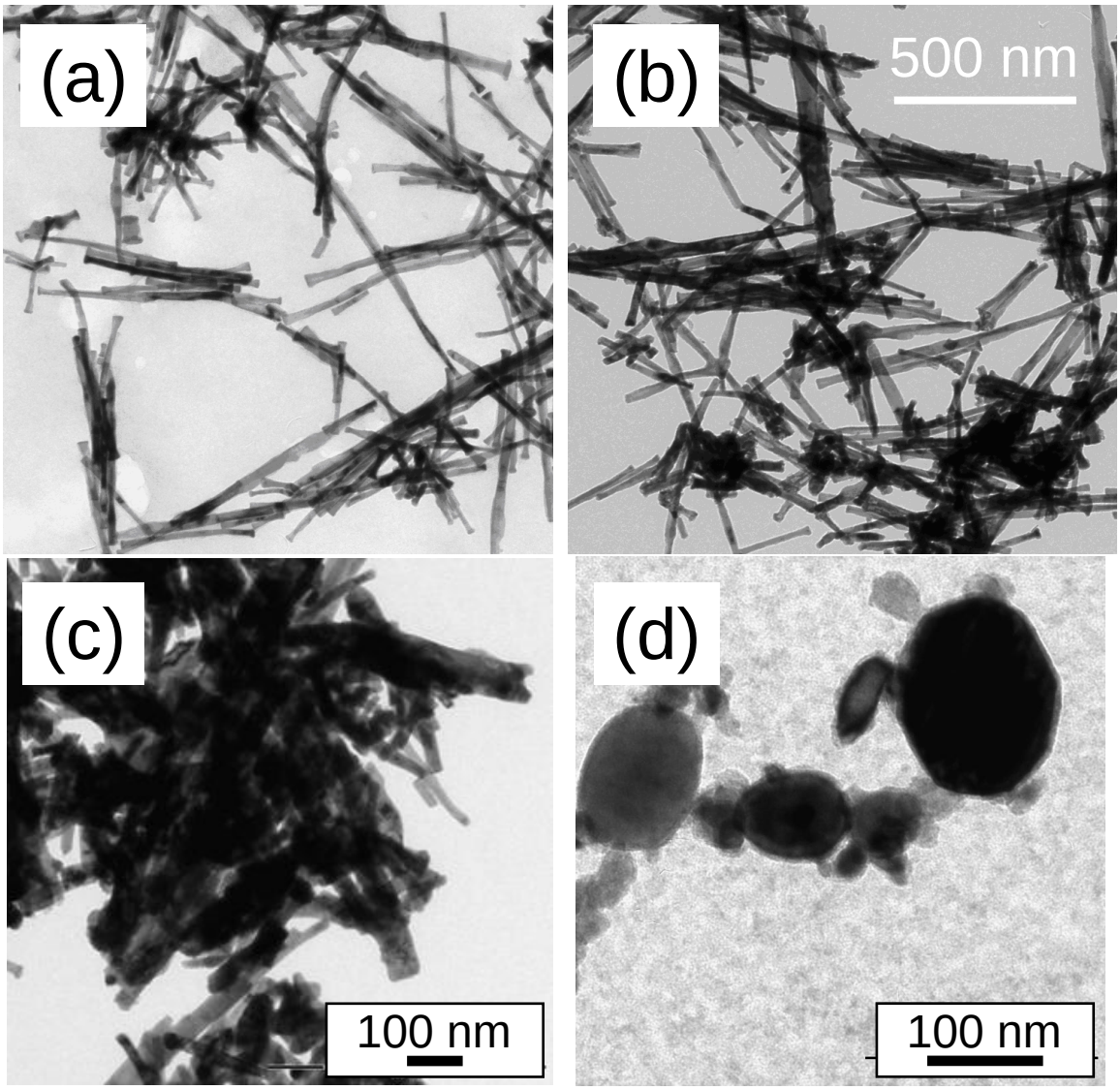

Figure 6.

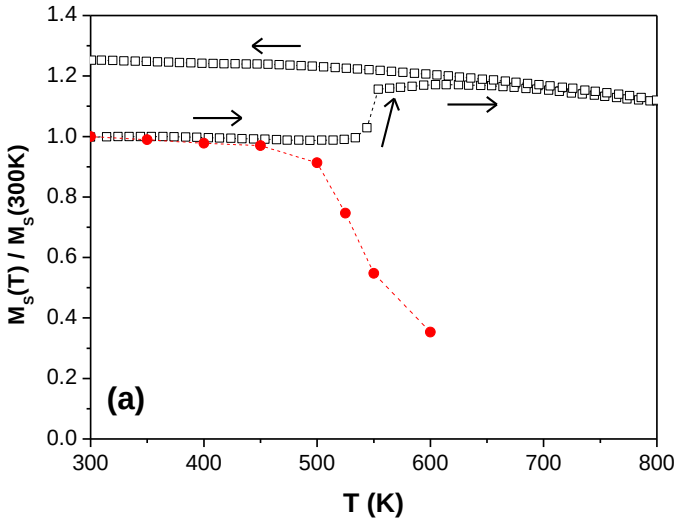
1.4
1.2
1.0
0.8
0.6
0.4
0.2
0.0
$M_s(T) / M_s(300K)$
(a)
300
400
500
600
700
800
T (K)

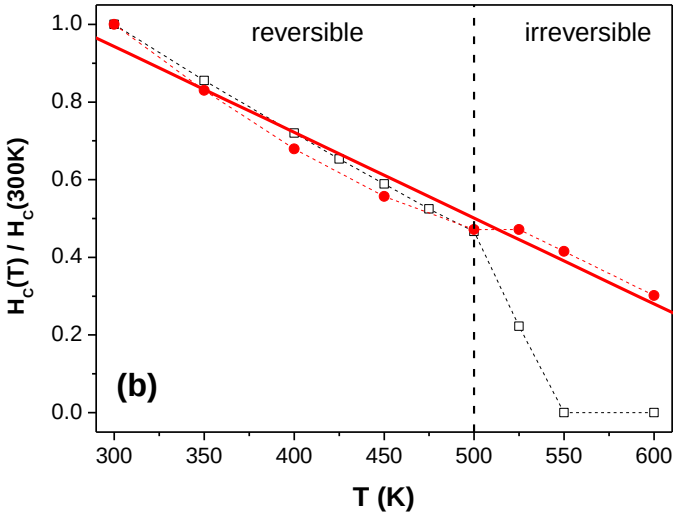
1.0
0.8
0.6
0.4
0.2
0.0
$H_c(T) / H_c(300K)$
reversible
irreversible
(b)
300
350
400
450
500
550
600
T (K)

Figure 7.

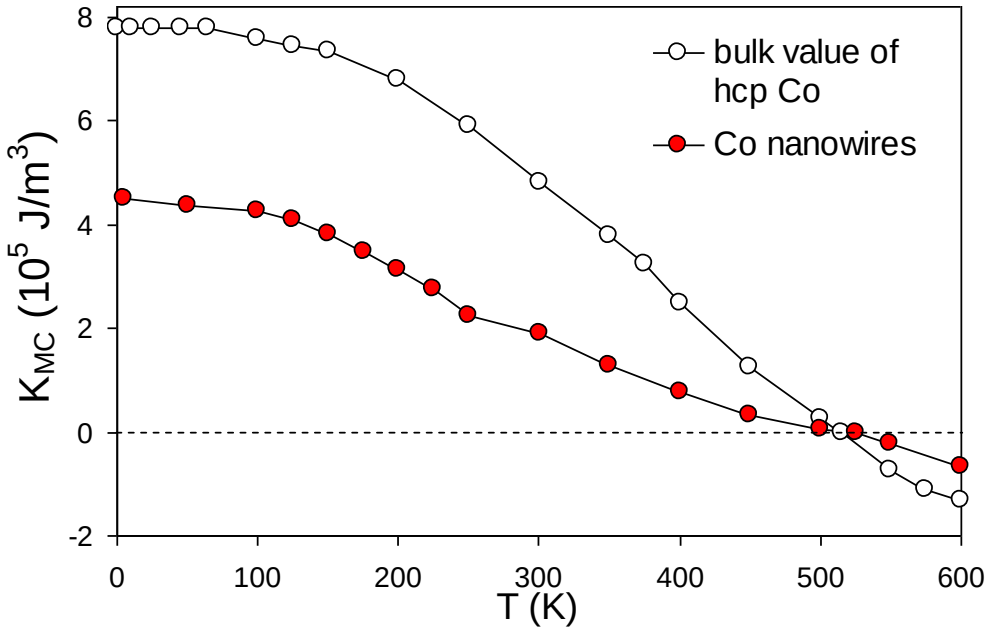
bulk value of
hcp Co
Co nanowires
K_{MC} (10^5 J/m^3)
T (K)
8
6
4
2
0
-2
0
100
200
300
400
500
600

Figure 8.